JOURNAL OF CATALYSIS 60, 276–294 (1979)

Characterization of Supported Molybdate Catalysts during Preparation Using Laser Raman Spectroscopy

C. P. CHENG AND G. L. SCHRADER[1]

Department of Chemical Engineering, University of Delaware, Newark, Delaware 19711

Received October 30, 1978; revised May 2, 1979

Laser Raman spectroscopy was used to investigate the formation of supported molybdate catalysts. Samples were prepared by the dry impregnation technique for the cobalt–molybdate hydrodesulfurization catalyst using γ-alumina, silica, and α-alumina supports. Variations in the preparation procedure were studied, including loadings of molybdenum and cobalt, order of impregnation, pH of impregnation solutions, and drying and calcining conditions. Spectra were recorded *in situ* using a rotating, controlled-atmosphere cell. Raman spectroscopy was demonstrated to be a very sensitive probe of the effect of variations in the preparation procedure. Spectra of dried samples indicated the presence of aggregated, distorted molybdenum species on all supports. Calcination of these samples resulted in the formation of "MoO_3" at higher molybdenum loadings; the presence of distorted molybdenum species showing high degrees of aggregation could be discerned for the silica and γ-alumina samples. Addition of cobalt to the molybdenum samples markedly changed the nature of the Raman spectra. The presence of "$CoMoO_4$" was observed; formation of this phase suppressed the formation of "MoO_3" until higher loadings were reached. Furthermore, addition of the cobalt tended to reduce the aggregation of the molybdenum surface species. Variation in the order of impregnation dramatically affected the relative amounts of surface molybdates as well as the aggregation of the surface species.

1. INTRODUCTION

The synthesis of active catalysts for specific chemical reactions typically involves a complex series of chemical and physical transformations, such as precipitation or impregnation, drying, calcining, and activation. The absence of fundamental information about catalyst preparation procedures is due, in part, to the difficulty of performing *in situ* studies of catalysts during preparation. This study has focused on the preparation procedure for the cobalt–molybdate hydrodesulfurization catalyst, using a technique which is well suited for studying catalyst preparation procedures—laser Raman spectroscopy.

Cobalt and molybdenum compounds supported on alumina are widely used as hydrodesulfurization catalysts. A wide variety of methods have been used to prepare these catalysts, with corresponding variations in activity, selectivity, and stability. Selection of the appropriate support has been studied by several workers (*1*) with alumina, silica-alumina, and silica receiving particular attention. Ahija *et al.* (*2*) studied the influence of the support on the hydrodesulfurization of a mixture of thiophene, toluene, and cyclohexane at 350°C and 60 kg/cm^2 H_2 pressure: Alumina and silica-alumina were found to be superior to silica as supports. DeBeer *et al.* (*3*), however, demonstrated that low loadings

---

[1] To whom correspondence should be addressed.

0021-9517/79/140276-19$02.00/0

of molybdenum on silica are comparable in activity to corresponding alumina-supported catalysts. Addition of cobalt resulted in an increase in activity of the molybdenum on alumina catalysts; molybdenum on silica catalysts exhibited an initial increase in activity followed by a significant deactivation. DeBeer reported some differences in the activity of catalysts using η- and γ-alumina supports, for short hydrodesulfurization times at 8 to 12 wt% molybdenum catalysts. Lo Jacono *et al.* (*4*) reported a study in which Ga^{3+} ions were added to γ-alumina. A larger amount of Co^{3+} in tetrahedral sites for the "surface" spinel was observed due to the addition of Ga^{3+}.

Differences in the activity of hydrodesulfurization catalysts also result from the various methods of incorporating the cobalt and molybdenum components, i.e., impregnation, precipitation, or mechanical mixing. Mechanical mixtures of alumina, cobalt oxide, and molybdenum oxide are convenient for catalyst manufacture, but the resulting catalyst is not very active. Coprecipitation of cobalt and molybdenum oxides in the presence of a freshly prepared alumina slurry or coprecipitation of all components result in more active catalysts. However, the most frequently described method for preparing cobalt molybdenum catalysts is the impregnation of the dry alumina support with solutions of cobalt and molybdenum salts. The sequence of adding the impregnation solutions is also recognized as being important in determining the ultimate activity and selectivity of the catalyst. "Wet impregnation" techniques have been used in which the support is immersed in an excess of solution which is subsequently drained away. "Dry impregnation" involves addition of sufficient solution to fill the pore volume of the alumina.

The use of Raman spectroscopy to characterize the oxidic form of cobalt–molybdenum catalysts has been described in the literature (*5–8*). Although the Raman technique details the complex structure of the supported molybdenum oxide, no study of the effect of preparation procedures on the catalyst structure has been reported. In this study, the effect of several important preparation parameters have been investigated, including type of support, pH of impregnation solutions, order of impregnation, and drying and calcining conditions.

2. EXPERIMENTAL METHODS

2a. Instrumentation

Raman spectra were recorded on a Spex Ramalog 5 spectrometer. The monochromator was equipped with holographic gratings; a "third monochromator" was also available with this instrument. A Spectra-Physics Model No. 164 Ar^+ laser was used as the excitation source for most experiments with an intensity of approximately 200 mW, measured at the source. Slit width settings corresponded to 4 cm^{-1} resolution for the 488.0-nm line. Signal detection was achieved with an RCA C31034 GaAs photomultiplier tube which was cryogenically cooled to -30°C. Photon-counting detection was used exclusively.

A Nicolet 1180 data system was directly interfaced to the Raman spectrometer and was used for routine data processing, including spectral accumulation, subtraction, and Fourier transformation.

2b. Rotating Controlled Atmosphere Cell

In order to record *in situ* spectra during catalyst preparation under a controlled environment, a rotating cell was designed (*9*, *10*). Samples, pressed into the form of pellets, were rotated at speeds of approximately 1500 rpm to minimize sample heating and/or degradation. The sample cell was capable of withstanding temperatures in the -60 to 600°C range in the spectrometer, and vacuums of 10^{-6} Torr

TABLE 1

Raman Spectra of Dried Co–Mo/γ–Al_2O_3 (cm^{-1})

Sample	0–200	201–400	401–600	601–800	801–1000	1000+
Mo(1.25)		327 w, br			926 s	
Mo(2.5)		215 w 330 w			935 s	
Mo(5)		213 w 334 w	563 vw		901 m, br 949 s	
Mo(10)	139 w	215 w 358 w	573 vw	740 vw	882 sh 901 m 926 sh 945 s	
Mo(15)	136 w	218 m 320 sh 360 m 378 w	580 w	741 w	878 sh 901 m 926 sh 949 s	
Mo(20)	138 w	218 m 362 m	580 w	730 vw	880 sh 903 m 923 sh 952 s	
Co(3)Mo(1.25)		250 w, br 350 w, br		692 m	842 w 940 m	1048 s
Co(3)Mo(2.5)		240 w, br 340 w, br		693 m	840 w 940 s	1050 s
Co(3)Mo(5)		223 w 351 m	562 vw	730 vw	819 m 875 sh 935 s 945 sh	1050 s
Co(3)Mo(10)		223 m 356 m	559 w	727 vw	812 m 868 sh 897 m 935 sh 943 s	1047 m
Co(3)Mo(15)	141 w	219 m 332 sh 355 m 381 sh	568 w	713 vw	807 sh 860 sh 901 m 939 sh 944 s	1048 w
Co(3)Mo(20)	137 w	221 m 335 sh 358 m 380 sh	574 w	617 sh 720 w	804 m 860 sh 901 m 935 sh 942 s 950 sh	1052 w
Mo(10)Co(3)	138 w	219 m 336 sh 358 m 379 sh	572 w	711 vw	815 m 855 m 898 m 935 sh 947 s	1048 m
Co(3)Mo(10) (simultaneous)	137 sh	221 m 330 sh 357 m	568 w	718 vw	805 m 848 m 899 m 934 s 941 sh	1048

could be achieved. Gases were passed through the sample cell via entrance and exit ports. An optically flat glass window was used for collection of scattered radiation, and the loss in intensity was observed to be minimal.

The sample cell was positioned in the sample compartment with a special mount designed to provide maximum stability and maneuverability. Five degrees of freedom are provided by the mount: translation parallel to the laser beam, translation parallel to the spectrometer axis, translation perpendicular to the plane containing the spectrometer axis and the laser beam, rotation about an axis of the laser beam, and rotation about an axis perpendicular to the laser beam.

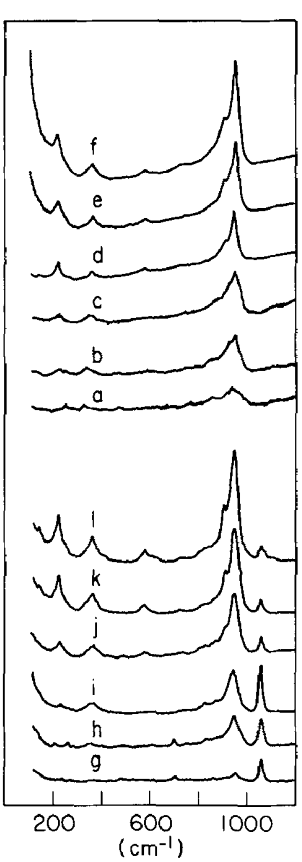

FIG. 1. Raman spectra of dried Co–Mo/γ-Al_2O_3. (a) Mo(1.25)/γ-Al_2O_3; (b) Mo(2.5)/γ-Al_2O_3 (c) Mo(5)/γ-Al_2O_3; (d) Mo(10)/γ-Al_2O_3; (e) Mo(15)/γ-Al_2O_3; (f) Mo(20)/γ-Al_2O_3; (g) Co(3)Mo(1.25)/γ-Al_2O_3; (h) Co(3)Mo(2.5)/γ-Al_2O_3; (i) Co(3)-Mo(5)/γ-Al_2O_3; (j) Co(3)Mo(10)/γ-Al_2O_3; (k) Co(3)Mo(15)/γ-Al_2O_3; (l) Co(3)Mo(20)/γ-Al_2O_3. Spectra a, b, c, g, h, i reported at 3× sensitivity as spectra d, e, f, j, k, l.

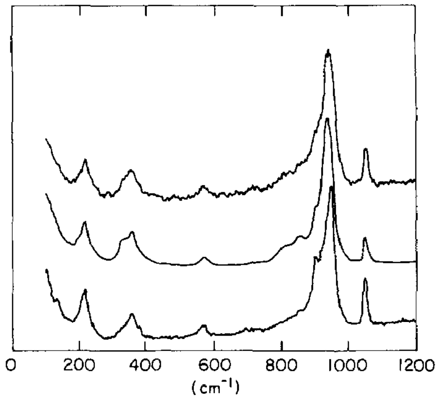

FIG. 2. Raman spectra of dried Co–Mo/γ-Al_2O_3; variations in order of addition. (a) Co(3)Mo(10)/γ-Al_2O_3, molybdenum impregnated first; (b) Co(3)-Mo(10)/γ-Al_2O_3, simultaneous impregnation; (c) Co(3)Mo(10)/γ-Al_2O_3, cobalt impregnated first.

2c. Catalyst Preparation

Catalysts were prepared by impregnation of cobalt and molybdenum solutions on the support using the "dry impregnation" technique. The general procedure may be described briefly as follows. Solutions were prepared from ammonium heptamolybdate [$(NH_4)_6Mo_7O_{24}\cdot 4H_2O$] (Fischer Scientific Co.) and cobalt nitrate [$Co(NO_3)_2\cdot 6H_2O$] salts (Fischer Scientific Co.); the pHs of these solutions were adjusted by addition of nitric acid or ammonium hydroxide. Samples were dried with air at 110°C for up to 4 hr. Calcination was performed at 500°C for up to 6 hr. These procedures could be performed in a drying oven and furnace or *in situ* with the Raman spectrometer.

Surface area measurements were performed with a Cahn microbalance. The surface areas of the supports were determined to be as follows: γ-alumina (BHD Chemicals, Ltd.), 101 m^2/g; α-alumina (Fischer Scientific Co.), 1.2 m^2/g; and

TABLE 2

Raman Spectra of Dried Co–Mo/γ-Al_2O_3 Impregnation with Solutions at Different pHs (cm^{-1})

Sample	0–200	201–400	401–600	601–800	801–1000	1000+
Mo(10) pH 9	139 w	218 m 352 m	562 w	740 w, br	840 sh 881 sh 893 m, sh 918 sh 940 sh 945 s	
Mo(10) pH 7	139 w	219 m 323 sh 353 m	577 w	750 w, br	840 sh 876 sh 899 s 920 sh 943 s	
Mo(10) pH 4	139 w	219 m 320 sh 356 m 379 sh	570 w	730 w, br	899 s 918 sh 947 s	
Co(3)Mo(10) pH 9	139 w	221 m 330 sh 355 m 375 sh	574 w	723 w, br	812 sh 860 sh 900 m 920 sh 935 s 947 sh	1050 m
Co(3)Mo(10) pH 7	140 w	222 m 330 sh 356 m 379 sh	570 w	716 w, br	814 sh 862 sh 899 sh 918 sh 935 sh 946 s	1049 m
Co(3)Mo(10) pH 4	139 w	221 m 320 sh 356 m 379 sh	570 w	730 w, br	815 sh 860 sh 898 m 935 sh 946 s	1049 m

silica gel (BDH Chemical, Ltd., chromatographic grade) 782 m^2/g.

3. EXPERIMENTAL RESULTS

3a. Dried Catalysts—Co–Mo/γ-Al_2O_3

The spectra of dried Mo/γ-Al_2O_3 at loadings of 1.25, 2.5, 5, 10, 15, and 20% (MoO_3) are summarized in Table 1 and in Fig. 1. The alumina background in these spectra is moderately fluorescent, although the intensity decreases substantially at higher molybdenum loadings, apparently due to some quenching of the fluorescence due to the molybdate species. A strong band at 950 cm^{-1} and a medium band at 901 cm^{-1} are present in the spectra of samples with loadings greater than Mo(5); less intense bands in the region of 215, 355, 570, and 735 cm^{-1} are apparent also. The spectrum of the sample with the lowest molybdenum loading has bands at considerably lower wavenumbers.

The spectrum of the dried samples are very similar to that of aqueous molybdenum solutions at low pHs. The spectrum of $Mo_7O_{24}^{6-}$ at pH 6.0 has bands at 219, 360, 474, 896, and 941 cm^{-1}. The corresponding bands for the supported molybdenum compounds are shifted higher

(570, 901, and 950 cm^{-1}) and lower (215 and 355 cm^{-1}). This general trend is also observed in aqueous solution as the pH is decreased. In general, the Raman bands of the supported species are also considerably broadened.

Addition of cobalt to molybdenum on alumina resulted in dramatic differences in the spectra, as indicated in Table 1. A characteristic nitrate peak is clearly present at 1045 to 1050 cm^{-1}; this peak persists after even longer periods of drying at 110°C. Considerable changes also occur in the 800 to 950 cm^{-1} region of the spectrum. Most striking is the appearance of new bands at 800 to 820, 860 to 875, and 935 to 950 cm^{-1}. At higher molybdenum loadings, some of these bands appear as shoulders. In addition, lower wavenumber bands near 221, 335, and 560 and 580 cm^{-1} are shifted from lines of molybdenum on alumina. A general decrease in bandwidth is also apparent in these spectra, observed more clearly in the low wavenumber region. These spectra match no known spectra of molybdenum compounds although they closely resemble spectra of precipitated molybdates.

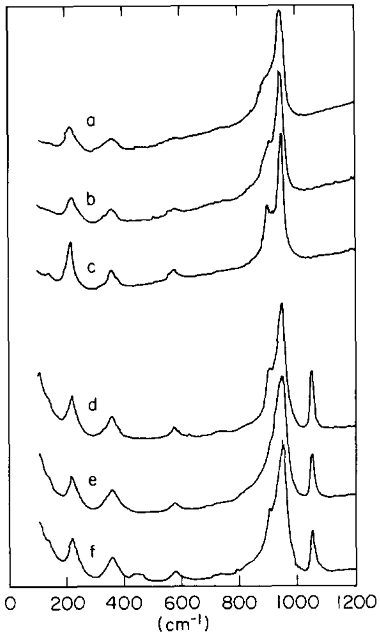

FIG. 3. Raman spectra of dried Co–Mo/γ-Al_2O_3; impregnation with solutions at various pHs. (a) Mo(10)/γ-Al_2O_3, pH 9; (b) Mo(10)/γ-Al_2O_3, pH 7; (c) Mo(10)/γ-Al_2O_3, pH 4; (d) Co(3)Mo(10)/γ-Al_2O_3, pH 9; (e) Co(3)Mo(10)/γ-Al_2O_3, pH 7; (f) Co(3)Mo(10)/γ-Al_2O_3, pH 4.

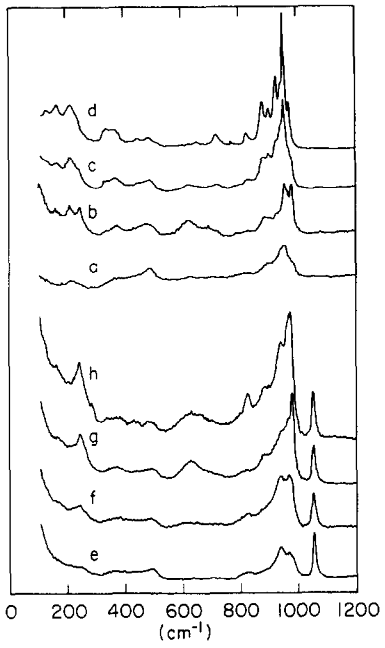

FIG. 4. Raman spectra of dried Co–Mo/SiO_2. (a) Mo(5)/SiO_2; (b) Mo(10)/SiO_2; (c) Mo(15)/SiO_2; (d) Mo(20)/SiO_2; (e) Co(3)Mo(5)/SiO_2; (f) Co(3)Mo(10)/SiO_2; (g) Co(3)Mo(15)/SiO_2; (h) Co(3)Mo(20)/SiO_2.

Addition of the cobalt solution prior to molybdenum results in the formation of different surface species, shown in Fig. 2. Raman bands are apparent at 815, 898, 947, and 1048 cm^{-1}. In addition, the bands tend to be much narrower and more well defined. Spectra of dried compounds prepared with a single solution of molybdenum and cobalt also differed from the spectra of the dried Co–Mo/γ-Al_2O_3 compounds. Peaks are observed at 137, 221, 330, 357, 568, 718, 899, and 1048 cm^{-1} while bands present at 805, 848, and 941 cm^{-1} are broadened. The band at 848 cm^{-1} is considerably lower than corresponding bands for spectra in which molybdenum

TABLE 3

Raman Spectra of Dried Co–Mo/SiO$_2$ (cm^{-1})

Sample	0–200	201–400	401–600	601–800	801–1000	1000+
Mo(5)		213 m 368 w, br	492 m	629 vw	805 sh 865 sh 895 m 932 sh 953 s	
Mo(10)	163 w	208 m 365 w, br	485 w	716 vw 627 w	838 w 879 sh 896 m 929 sh 953 s 970 sh	
Mo(15)	169 w	210 m 365 m, br	483 w	628 vw 720 w	835 w, br 882 sh 900 m 929 sh 952 s 968 sh	
Mo(20)	166 m	212 m 358 m, br	444 vw 483 w	642 w 709 m	821 m 879 m 900 m 926 s 945 sh 952 s 971 m	
Co(3)Mo(5)		223 vw 337 w, br	485 w	610 w	830 m 878 sh 910 sh 932 s 977 sh	1048 m
Co(3)Mo(10)		246 m 353 w	485 w	606 w	831 w 879 sh 926 s 935 sh 961 s 974 sh	1045 m
Co(3)Mo(15)	169 w	244 m 281 sh 340 w, br	485 w	623 w	820 m 878 sh 922 sh 938 sh 968 s 972 sh	1048 m
Co(3)Mo(20)	163 w	246 m 273 sh 335 w 382 w	476 w	628 m	821 m 882 sh 926 sh 937 sh 962 sh 975 s	1050 m

TABLE 3—*Continued*

Sample	0–200	201–400	401–600	601–800	801–1000	1000+
Mo(10)Co(3)	150 w	238 w 330 m 355 w	568 w	718 vw	800 m 825 sh 848 m 899 sh 934 s 942 sh 970 sh	1043 w
Co(3)Mo(10) (simultaneous)	172 w	250 w 265 sh 330 w 365 w	490 w	629 w	820 m, br 853 m, br 910 sh 929 sh 932 s 974 m	1048 m

was impregnated first. Even the most intense peak, the 934 cm^{-1} band, is anomolously low for these levels of molybdenum loading.

The spectra of dried Mo/γ-Al_2O_3 prepared from molybdenum at different pHs did not show fundamental differences (Table 2 and Fig. 3). However, there was a difference in the band width: Compounds prepared at high pHs show considerably broader bands centered at 950 cm^{-1}. In addition, there is considerable reduction in the intensity of low wavenumber bands in the spectra of compounds prepared at pHs of about 9. The presence of cobalt appears to moderate the effect of pH on the spectra of the surface species. These results are also given in Table 2. Addition of the cobalt at higher pHs appears to result in the decrease in the intensity and/or broadening of bands in the 800 to 840 cm^{-1} region. Thse results are particularly intriguing because of the presence of molybdenum exclusively as MoO_4^- tetrahedra at pHs greater than 8.

3b. Dried Catalysts—Co–Mo/SiO$_2$

Spectra of dried Mo/SiO_2 generally exhibit considerably more Raman bands than do spectra of Mo/γ-Al_2O_3 or aqueous molybdenum solutions. These spectra are summarized in Table 3 and Fig. 4. The silica used in these studies was less fluorescent than the γ-alumina and had a considerably higher surface area. A large number of bands are apparent, and although the spectrum resembles ammonium paramolybdate, the position of the bands extends over a much larger spectral region. Bands are present for the supported molybdate which are at much higher wavenumbers, e.g., 953 to 975 cm^{-1}, and lower wavenumbers, e.g., 821 cm^{-1}. The low wavenumber region of the spectrum is typically quite well defined at low loadings of molybdenum. This region of the spectrum is dominated by a silica band at about 485 cm^{-1}, but a band at 213 cm^{-1} is also observed. Additional bands can be observed at higher molybdenum loadings. Most of these bands are only moderately broader than those of ammonium paramolybdate.

Addition of cobalt results in several significant changes in the spectrum. At low molybdenum levels, the strongest peak is at 932 cm^{-1} with a shoulder at 977 cm^{-1}; the latter band is more intense for samples which have a higher molybdenum loading. At the highest loading of molybdenum, this band appears as a doublet at 962 and 975 cm^{-1}. In addition, numerous other bands are observed in the 800 to 900 cm^{-1}

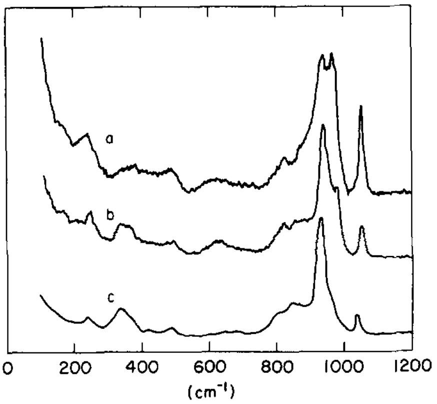

FIG. 5. Raman spectra of dried Co–Mo/SiO_2; variations in order of addition. (a) Co(3)Mo(10)/SiO_2, molybdenum impregnated first; (b) Co(3)-Mo(10)/SiO_2, simultaneous impregnation; (c) Co(3)-Mo(10)/SiO_2, cobalt impregnated first.

region which are quite narrow and well defined. This is not true, however, of the low wavenumber region; most of the bands in this region are very broad and weak.

The order of impregnation also radically changes the character of the spectrum (shown in Fig. 5). Lines observed at 800, 825, and 848 cm^{-1} are significantly lower for samples impregnated with cobalt first; lower wavenumber bands generally are shifted also to lower wavenumbers. In addition, the relative intensities of the bands is dramatically different.

3c. *Dried Catalysts—Co-Mo/α-Al_2O_3*

The spectra of Mo/α-Al_2O_3 at different molybdenum loadings have several peaks consistent with ammonium heptamolybdate: 948 and 882 cm^{-1} for Mo/α-Al_2O_3 and 938 and 888 to 893 cm^{-1} for ammonium paramolybdate. A lower band is present at 840 cm^{-1}. The low wavenumber bands of the spectrum are remarkably broad for this low surface area compound. At higher molybdenum loadings, a sharp strong band at 950 cm^{-1} appears with an improvement in the sharpness of the lower wavenumber vibrations.

Addition of cobalt to Mo/α-Al_2O_3 results in a broadening of most bands in the spectra; the bands in the 800 to 950 cm^{-1} region are particularly broad and several of the most intense bands of the Mo/α-Al_2O_3 species are missing, e.g., 970 and 950 cm^{-1}. Order of impregnation is important, as these higher wavenumber bands are present in samples in which cobalt has been impregnated prior to molybdenum.

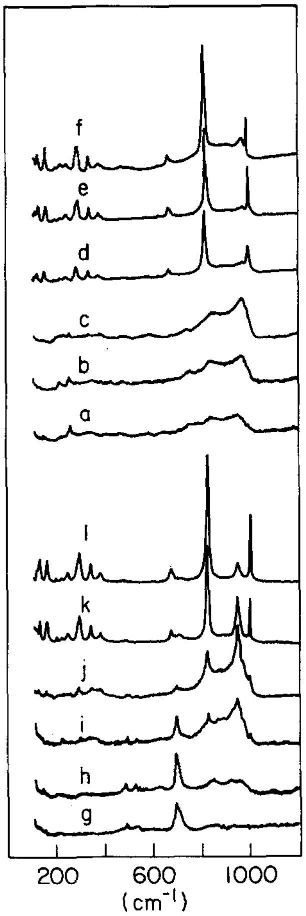

FIG. 6. Raman spectra of calcined Co–Mo/γ-Al_2O_3. (a) Mo(1.25)/γ-Al_2O_3; (b) Mo(2.5)/γ-Al_2O_3; (c) Mo(5)/γ-Al_2O_3 (d) Mo(10)/γ-Al_2O_3; (e) Mo(15)/γ-Al_2O_3; (f) Mo(20)/γ-Al_2O_3; (g) Co(3)-Mo(1.25)/γ-Al_2O_3; (h) Co(3)Mo(2.5)/γ-Al_2O_3; (i) Co(3)Mo(5)/γ-Al_2O_3; (j) Co(3)Mo(10)/γ-Al_2O_3; (k) Co(3)Mo(15)/γ-Al_2O_3; (l) Co(3)Mo(20)/γ-Al_2O_3. Spectra a, b, c, g, h, i reported ad 3× sensitivity as d, e, f, j, k, l.

3d. Calcined Catalysts—Co-Mo/γ-Al_2O_3

The results of calcined samples of molybdenum at various loadings are given in Table 4 and Fig. 6. At low loadings of molybdenum the spectral features which are observed are quite broad and are of low intensity. Bands are observed at approximately 220, 320 to 350, 838, and 943 cm^{-1}, with an additional broad shoulder in the 900 to 930 cm^{-1} region. The spectrum of this molybdate species is considerably different than that of samples prepared at higher molybdenum loadings. For these samples, bands characteristic of MoO_3 are present at 995, 819, and 664 cm^{-1}, which are only slightly shifted from the pure compound (996, 821, and 668 cm^{-1}). Rather large shifts occur in the low wavenumber region, particularly at low molybdenum loadings. The existence of broad bands in the intermediate region, 830 to 970 cm^{-1}, is observed in all spectra. Very significant shifts in the frequencies of these bands occur as a function of molybdenum loading.

Addition of cobalt to Mo/γ-Al_2O_3 results in the formation of new surface compounds, indicated by new bands appearing at about 939, 697, 527, and 481 cm^{-1}. These band positions are similar to those for β-$CoMoO_4$ (purple) and Co_3O_4, although the displacements of the bands are significant as are the changes in relative intensity. Bands attributable to a "MoO_3" phase are also present at 995, 818, and 667 cm^{-1}. In addition, a broad band is present in the 820 to 950 cm^{-1} region. The low wavenumber region is rather poorly defined until higher levels of molybdenum are reached.

Reversal of the order of impregnation of molybdenum and cobalt leads to a much different spectrum (Fig. 7). A peak indicative of a "Co_3O_4" phase is present at 694 cm^{-1}. The relative amount of "MoO_3" is also higher, but there has been significant decrease in the peak at 942 cm^{-1}. On the other hand, simultaneous addition of cobalt and molybdenum results in the surface composition dominated by the "$CoMoO_4$" band at 939 cm^{-1} and the "Co_3O_4" band at 699 cm^{-1}.

Spectra of Mo/γ-Al_2O_3 and Co-Mo/γ-Al_2O_3 showed some differences as a function of pH (Table 5 and Fig. 8). The changes are apparent in the 900 to 985 cm^{-1} region of the spectrum. A gradual shift in wavenumber position toward lower wavenumbers occurs as the pH decreases. In addition, the sharpness of the bands improves, and additional side bands can be distinguished. The effect of pH on Co-Mo/γ-Al_2O_3 is more difficult to discern, partially because of the more intense band at 940 cm^{-1}. However, an effect on the relative amounts of "MoO_3" and "$CoMoO_4$" is apparent.

3e. Calcined Catalysts—Co-Mo/SiO_2

Spectra of calcined Mo/SiO_2 (Table 6 and Fig. 9) indicate the presence of a "MoO_3" phase by lines at 994, 817, and 669 cm^{-1}. In addition, there is a band at 950 to 980 cm^{-1} which is the most intense feature of the spectrum at low levels of molybdenum loadings. This is also true of broad band in the 855 to 880 cm^{-1} region; in fact several distinct bands are observable in this region. These samples generally exhibit rather well-defined low wavenumber bands at lower molybdenum loadings than do the γ-Al_2O_3 samples.

Introduction of cobalt into these samples results in the formation of a "$CoMo_4$" phase with a characteristic band at 939 cm^{-1}. Addition of cobalt dramatically decreases the amount of "MoO_3" ultimately present in the sample. There are also additional weak bands present in the intermediate 820 to 920 cm^{-1} region which results in a rather broad band. This feature is more apparent in the spectra of samples with low molybdenum loadings. Reversal of the order of impregnation of cobalt and molybdenum alters the amount of

TABLE 4

Raman Spectra of Calcined Co–Mo/γ–Al_2O_3 (cm^{-1})

Sample	0–200	201–400	401–600	601–800	801–1000	1000+
Mo(1.25)		223 w 322 w			838 m 943 s	
Mo(2.5)		220 w 350 w			853 m 944 s	
Mo(5)		219 w 354 w			819 w 907 m 952 s	
Mo(10)	114 m 124 m 155 m 193 w	213 w 242 w 287 m 378 m	470 vw	664 m	815 s 915 w 967 m 995 s	
Mo(15)	118 w 128 m 158 m 199 w	218 w 243 w 289 m 337 m 378 w	470 vw	665 m	819 s 920 w 970 m 995 s	
Mo(20)	117 w 129 m 157 m 200 w	218 w 246 w 290 m 339 m 379 w	471 vw	667 w	819 s 922 w 972 sh 996 s	
Co(3)Mo(1.25)			481 w 523 w	697 s		
Co(3)Mo(2.5)			486 w 527 w	694 s	846 m 913 m 948 m	
Co(3)Mo(5)		224 vw 339 w, br		690 m	817 s 870 br 910 m, br 939 s 994 m	
Co(3)Mo(10)	127 w 158 w	287 w 339 w 369 w		690 w	818 s 867 br 912 m, br 938 s 949 sh 994 m	
Co(3)Mo(15)	116 w 126 m 157 m 195 vw	220 vw 243 w 290 m 337 m 378 w	473 vw	667 m 700 m	818 s 867 br 940 m 949 sh 995 m	
Co(3)Mo(20)	117 w 129 m 157 m 197 vw	218 w 245 w 292 m 339 m 378 w	473 vw	667 m	818 s 940 m 949 sh 994 m	

TABLE 4—*Continued*

Sample	0-200	201-400	401-600	601-800	801-1000	1000+
Mo(10)Co(3)	116 w 127 m 157 m 198 vw	218 vw 243 w 289 m 336 m 379 w	475 vw	666 m 694 w	817 s 945 w 995 m	
Co(3)Mo(10) (simultaneous)	116 w 127 w 158 w	218 vw 224 w 290 m 336 w 375 w	480 vw	667 w 701 m	817 m 890 br 939 s 946 sh 994 m	

"CoMoO$_4$" formed; the Raman spectrum indicates the presence of considerably more "CoMoO$_4$" as well as the presence of a "Co$_3$O$_4$" phase (see Fig. 10).

3f. *Calcined Catalysts—Co-Mo/α-Al$_2$O$_3$*

The Raman spectra of Mo/α-Al$_2$O$_3$ after calcining demonstrates clearly the presence of MoO$_3$ with lines at 996, 819, and 667 cm^{-1}. The spectra of samples with different loadings of Mo are very similar, which is not surprising because of the low surface area of these samples. At these levels of molybdenum loadings, there is no appearance of any bands in the intermediate 840 to 980 cm^{-1} region.

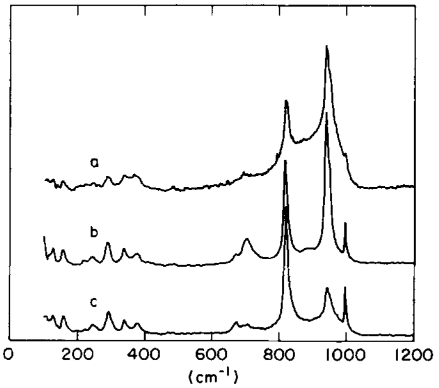

FIG. 7. Raman spectra of calcined Co–Mo/γ-Al$_2$O$_3$; variations in order of addition. (a) Co(3)-Mo(10)/γ-Al$_2$O$_3$, molybdenum impregnated first; (b) Co(3)Mo(10)/γ-Al$_2$O$_3$, simultaneous impregnation; (c) Co(3)Mo(10)/γ-Al$_2$O$_3$, cobalt impregnated first.

Addition of cobalt to these samples results in the appearance of a "CoMoO$_4$" phase whose most intense line closely coincides with that of β-CoMoO$_4$.

4. DISCUSSION OF RESULTS

Molybdenum compounds, like those of tungsten and uranium, are noted for their wide variation in stereochemistry and oxi-

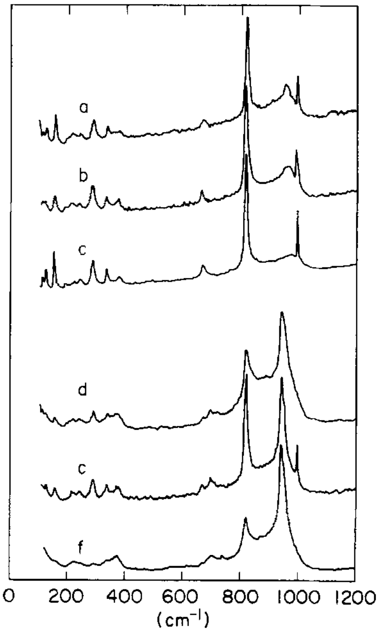

FIG. 8. Raman spectra of calcined Co–Mo/γ-Al$_2$O$_3$; impregnation with solutions at different pHs. (a) Mo(10)/γ-Al$_2$O$_3$, pH 9; (b) Mo(10)/γ-Al$_2$O$_3$, pH 7; (c) Mo(10)/γ-Al$_2$O$_3$, pH 4; (d) Co(3)Mo(10)/γ-Al$_2$O$_3$, pH 9; (e) Co(3)Mo(10)/γ-Al$_2$O$_3$, pH 7; (f) Co(3)Mo(10)/γ-Al$_2$O$_3$, pH 4.

TABLE 5

Raman Spectra of Calcined Co–Mo/γ-Al_2O_3 Impregnation with Solutions at Various pHs (cm^{-1})

Sample	0–200	201–400	401–600	601–800	801–1000	1000+
Mo(10)	115 w	218 w		669 w	819 s	
pH 9	129 w	291 w			930 w	
	157 w	340 w			952 m	
	196 w	375 w			994 s	
Mo(10)	122 w	214 w		668 w	816 s	
pH 7	157 w	241 w			940 w	
		282 m			954 m	
		332 w			993 s	
		374 w				
Mo(10)	119 w	218 w		669 w	819 s	
pH 4	129 w	245 w			961 m	
	158 w	290 m			995 m	
	195 w	337 w				
		387 w				
Co(3)Mo(10)	155 w	221 w		665 w	819 s	
pH 9		244 w		691 w	938 s	
		292 w			948 sh	
		339 w			994 m	
		367 w				
Co(3)Mo(10)	128 w	224 w		666 w	817 s	
pH 7	158 w	245 w		694 w	939 s	
		293 w			948 sh	
		339 w			995 m	
		377 w				
Co(3)Mo(10)	158 w	221 w		665 w	819 s	
pH 4		289 w		669 w	939 s	
		337 w			949 sh	
		377 w			994 m	

dation state. This complex character is well represented by the oxygen compounds of molybdenum, among which is the oxidic precursor of the cobalt–molybdate hydrodesulfurization catalyst. Vibrational spectroscopy has been demonstrated to be a valuable probe of the structure of molybdate compounds since the coordination of solid-state compounds is closely related to their infrared and Raman spectra (*11*). This is particularly true for Raman spectroscopy because of the definition of the Raman lines and the strong scattering properties of the oxides. The Raman spectra of molybdate compounds which are particularly important in this study are summarized in Table 7. The assignment of the vibrational lines is not unambiguous, however: The ranges of frequencies for tetrahedral and octahedral Mo–O bond stretches frequently overlap. Moreover, the structure of many molybdate compounds cannot be classified as having precisely octahedral or tetrahedral coordination of the molybdenum ions. Since such structures are likely to be very important in catalysis by supported molybdate species, a study of the structure and coordination of supported molybdate compounds was performed.

In order to understand better the nature of the cobalt–molybdate catalyst structure and chemistry, the most readily characterized molybdates, those formed in aqueous solution, were studied. Molybdenum ions are known to form isopolyanions in aqueous solution, and the state of aggregation in these solutions is highly dependent on pH and concentration. In alkaline solutions, the predominant species is the MoO_4^{2-} species which clearly is tetrahedral with bond lengths of 1.76 Å (*12*). This spectrum has three clearly distinct bands at 896, 843, and 317 cm^{-1} (see Fig. 11). Four bands are predicted to be present in the Raman according to group theory [$\nu_1(A_1)$, $\nu_2(E)$, $\nu_3(T_2)$, and $\nu_4(T_2)$]; Busey and Keller (*13*) explained this discrepancy as due to low intensity of the $\nu_2(E)$ line. Upon acidification of MoO_4^{2-} solutions, a polymeric $Mo_7O_{24}^{6-}$ species is produced; these species exist simultaneously in solution over a quite broad pH range. The $Mo_7O_{24}^{6-}$ structure has been discussed analogously with the ammonium paramolybdate structure which consists of seven MoO_6 octahedra sharing edges (*14*). These octahedra have been clearly shown to be distorted, however (*15*, *16*). The Raman spectrum of the aqueous $Mo_7O_{24}^{6-}$ species has major bands at 219, 360, 474, 896, and 941 cm^{-1} while the spectrum of the solid ammonium paramolybdate has considerably more bands. The low wavenumber region of the spectrum particularly exhibits a large number of distinct bands, characteristic of the crystalline structure of the compound. Site symmetry splitting also is apparent in the 800 to 950 cm^{-1} region of the spectrum. Further acidification of aqueous solutions results in higher polymeric species such as $Mo_8O_{26}^{4-}$ along with other protonated species. The $Mo_8O_{26}^{4-}$ species also consists of corner-sharing molybdenum octahedra. Raman bands for the $Mo_8O_{26}^{4-}$ species occur at 210, 360, 910, and 958 cm^{-1}. Higher polymers are formed as more acid is added to aqueous solutions, and precipitation of highly aggregated species eventually occurs. Raman spectra of these solutions and the wet precipitates have well-defined bands; few other techniques have been used to characterize the species formed, although molecular weight and potentiometric measurements indicate the presence of approximately $Mo_{19}O_{59}^{4-}$ species (*17*, *18*).

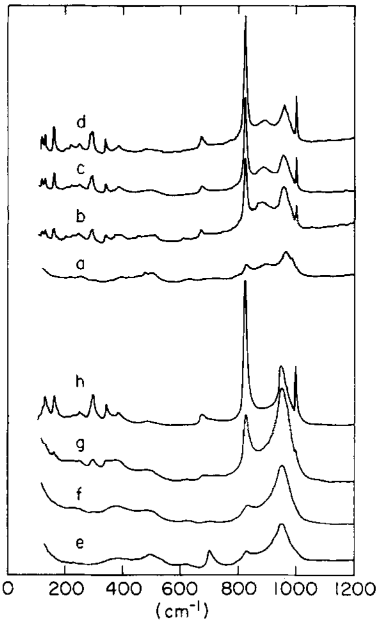

FIG. 9. Raman spectra of calcined Co–Mo/SiO_2. (a) Mo(5)/SiO_2; (b) Mo(10)/SiO_2; (c) Mo(15)/SiO_2; (d) Mo(20)/SiO_2; (e) Co(3)Mo(5)/SiO_2; (f) Co(3)Mo(10)/SiO_2; (g) Co(3)Mo(15)/SiO_2; (h) Co(3)Mo(20)/SiO_2.

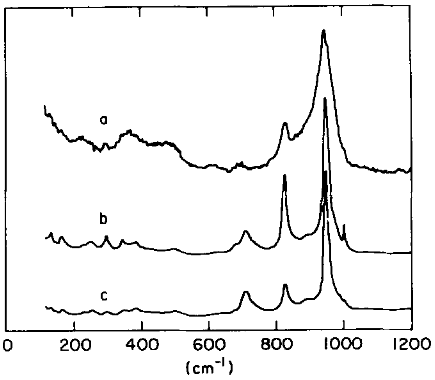

FIG. 10. Raman spectra of calcined Co–Mo/SiO_2; variations in order of addition. (a) Co(3)Mo(10)/SiO_2, molybdenum impregnated first; (b) Co(3)-Mo(10)/SiO_2, simultaneous impregnation; (c) Co(3)-Mo(10)/SiO_2, cobalt impregnated first.

TABLE 6

Raman Spectra of Calcined Co–Mo/SiO_2 (cm^{-1})

Sample	0–200	210–400	401–600	601–800	801–1000	1000+
Mo(5)	167 vw	246 w, br	492 w	610 vw	817 m	
		381 w, br		774 vw	883 m	
					951 s	
					981 sh	
					995 w	
Mo(10)	115 w	216 w	483 w	669 w	817 s	
	128 w	245 w			856 m	
	158 m	289 m			876 m	
	195 w	339 w			949 s	
		381 w, br			975 sh	
					994 m	
Mo(15)	117 m	216 w	492 w	662 m	819 s	
	128 m	246 w			856 m	
	160 m	292 m			881 m	
	198 w	337 m			952 m	
		378 w			981 sh	
					995 m	
Mo(20)	117 m	221 w	467 w	664 m	817 s	
	128 m	246 w			856 m	
	157 m	290 m			876 m	
	195 w	337 m			949 m	
		378 w			981 sh	
					995 m	
Co(3)Mo(5)		208 w	407 w	603 vw	815 w	
		342 w	486 m	693 m	880 sh	
					918 sh	
					940 s	
Co(3)Mo(10)		221 w	489 w	614 vw	817 m	
		346 w		695 vw	865 sh	
					934 sh	
					940 s	
					996 sh	
Co(3)Mo(15)	117 w	224 w	478 w, br	611 vw	819 s	
	128 w	249 w		669 w	895 sh	
	158 w	289 m			906 sh	
	198 w	337 w			932 s	
		375 w			953 sh	
					995 m	
Co(3)Mo(20)	117 w	221 w	471 w,br	666 w	820 s	
	128 m	242 w			882 w	
	158 m	292 m			920 sh	
	199 w	337 m			940 s	
		379 w			952 sh	
					995 s	
Mo(10)Co(3)	125 vw	222 w	478 w, br	609 vw	817 m	
	156 w	247 w		698 m	875 m	
		288 w			925 sh	
		339 w			940 s	
		374 w			946 sh	
					980 sh	
					995 m	

TABLE 6—*Continued*

Sample	0–200	210–400	401–600	601–800	801–1000	1000+
Co(3)Mo(10) (simultaneous)	118 w	227 w	482 w, br	667 w	819 s	
	128 w	242 w		700 m	882 m	
	158 m	290 m			939 s	
		339 w			944 sh	
		377 w			995 m	

Raman bands corresponding to the polarized $\nu_1(A_1)$ vibration were observed at 961, 976, and 983 cm^{-1} for solutions and wet precipitates and will be the subject of a separate discussion. However, a particularly well-defined model for higher aggregates of molybdenum exists; the heteropoly acids of molybdenum, namely, H_3 $PMo_{12}O_{40}$. The high wavenumber portion of this spectrum is also shown in Fig. 11, with bands appearing at 156, 248, 373, 467, 603, 715, 898, 975, 988, and 995 cm^{-1}. The 1:12 heteropolymolybdate consists of 12 octahedrally coordinated molybdenum atoms grouped around a tetrahedrally coordinated P^{5+} atom.

The metal–oxygen stretching vibration region of the spectrum of all of these compounds is remarkably similar. A sharp, intense band and a less intense, broad band are present in all spectra with the most striking difference being the position of the bands, i.e., larger aggregates of molybdenum have bands at higher wavenumbers. The relative position of the weaker band is an indication of the distortion of molybdenum environment (*13*). This $\nu_3(T_2)$ band appears to be sensitive to the environment of the molybdenum species. Lower wavenumber bands, in the metal–oxygen bridging region, also provide complementary information about the dis-

TABLE 7

Raman Spectra of Model Solid-State Compounds (cm^{-1})

Compounds	0–200	201–400	401–600	601–800	801–1000	1000+
$(NH_4)_6Mo_7O_{24}\cdot 4H_2O$	115 m	224 m	543 w	625 w	863 sh	
	135 m	252 m	570 w	633 w	888 m	
	199 m	308 w			893 m	
		339 w			908 sh	
		363 m			920 sh	
		375 m			938 s	
MoO_3	84 w	219 vw	472 vw	668 w	821 s	
	100 w	246 w		711 vw	849 vw	
	117 m	285 m		775 vw	996 m	
	130 m	293 m				
	159 m	338 w				
	198 vw	356 vw				
		369 w				
$CoMoO_4$		336 m	467 vw		806 m	
		358 m			852 m	
					935 s	
Co_3O_4		203 m	487 m	625 w		
			528 m	696 s		
$Al_2(MoO_4)_3$	139 vw	381 m	437 vw		830 w	1004 s
					891 vw	1027 m

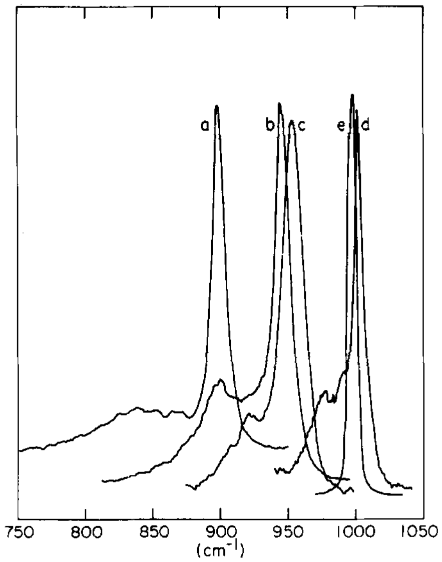

FIG. 11. Raman spectra of molybdenum aggregates. (a) MoO_4^{2-} (aqueous solution); (b) $Mo_7O_{24}^{6-}$ (aqueous solution); (c) $Mo_8O_{26}^{4-}$ (aqueous solution); (d) $PMo_{12}O_{40}^{3-}$ (aqueous solution); (e) MoO_3 (solid).

tortion and aggregation of the molybdenum species.

The lattice phonon region of the spectrum (typically less than 200 cm^{-1}) could be recorded for most supported molybdenum samples. The intensity and definition of bands in this region was related to the composition of the sample as well as to the preparation procedure. This region of the spectrum is most closely related to deviations from ideal crystal structure, such as nonstoichiometry and defect structures.

4a. Co–Mo/γ-Al$_2$O$_3$ Catalysts

The Raman spectra of dried and calcined Co–Mo/γ-Al_2O_3 demonstrate the sensitivity of the technique to the variations of molybdenum coordination and chemical state. More bands are apparent in the metal–oxygen stretching region for dried samples than for calcined samples. Repeated scans of different scanning speeds and slit widths and spectral accumulation indicated that the shoulders were valid spectral features. The appearance of the bands was very dependent on the preparation procedure, particularly the drying and calcining procedures.

Spectra of dried Mo/γ-Al_2O_3 indicate that a highly distorted molybdenum species is present on the γ-Al_2O_3 surface. This species resembles a corner-sharing aggregate, similar in coordination to the isopolyanion compounds ($Mo_7O_{24}^{6-}$ or $Mo_8O_{26}^{4-}$). The broad spectral features indicate distortion due to the γ-Al_2O_3 surface. The resemblance to the ammonium paramolybdate spectrum is more apparent at higher molybdenum loadings; however, even the spectrum for the lowest molybdenum loadings indicate the presence of an aggregated molybdenum species. Interestingly, the spectra do not indicate a strong effect of pH on the structure of the supported compound, even though the aqueous impregnation solutions differ greatly in the coordination of the molybdenum compounds. These results indicate that the interaction between the molybdenum species and the alumina surface strongly affects the degree of aggregation. Calcination of these compounds results in the formation of several molybdenum surface compounds which may be distinguished by the position of the Mo–O stretching vibrational band (the highest or "$\nu_1(A_1)$" band). Formation of a "MoO_3" phase does occur after a half monolayer equivalent of molybdenum on alumina has been added. The spectra of the calcined samples at low molybdenum loading are similar to the spectra of dried samples. The sharpness of the bands improves in the calcined form, indicating formation of a more ordered compound. A significant upward shift in the Mo–O stretching vibrational band occurs with an increasing in molybdenum loading, indicating the presence of more highly aggregated molybdenum species. In addition, the shift of the broad "$\nu_3(T_2)$" band parallels this upward shift of the "$\nu_1(A_1)$" band. The series of spectra attributed to the aggregated species then closely resemble the series shown in Fig. 11 for the isopolyanions. No bands attributable to bulk aluminum molybdate were observed.

Addition of cobalt nitrate solutions to the surface molybdenum compounds results in very clear changes in molybdenum compound structure and environment. Dried samples indicate a difference in the environment of a portion of the molybdenum species. In general, the bands are more well defined for the lower loadings of molybdenum such that Mo–O–Mo bringing vibrations are apparent at lower wavenumbers. The ability of the cobalt species to interact with the surface so as to modify the molybdenum–alumina interaction is apparent in Fig. 2, where the order of addition of molybdenum and cobalt is varied. Samples prepared by addition of cobalt prior to molybdenum show a more highly aggregated molybdenum species (i.e., 947 vs 943 cm^{-1} and a strong band at 898 cm^{-1}). In these spectra, the presence of lower stretching vibrations at 805 and 848 cm^{-1} is more clearly present; this difference is also apparent in the calcined form. Isolated molybdenum species are apparently indicated by these bands which ultimately produce a "$CoMoO_4$" phase. Calcination of all samples resulted in the formation of some "MoO_3" although addition of cobalt suppresses the formation of this phase until higher molybdenum loadings are reached. This is apparent in the samples prepared by changing the order of cobalt and molybdenum impregnation. Cobalt which has been incorporated into the alumina lattice does not readily form a "$CoMoO_4$" phase. The spectra of the "$CoMoO_4$" phase does not precisely resemble that of a bulk β-$CoMoO_4$; a shoulder at higher wavenumbers is present due to associated molybdenum oxide species. As for the molybdenum on alumina samples, the presence of a bulk alumina phase was not observed.

4b. Co–Mo/SiO_2 Catalysts

Raman spectra of molybdenum on silica generally had a larger number of well-defined bands than comparable γ-Al_2O_3 compounds. This occurs despite the much higher surface area of the silica. Many of these bands are shoulders until higher molybdenum loadings are reached. The aggregation of the molybdenum species is also clearly indicated by the appearance of bands at lower wavenumbers which appear much more readily than for γ-Al_2O_3. The splitting of bands also occurs for ammonium paramolybdate: This site symmetry splitting is indicative of the strong interactions between molybdenum species. These interactions are expected to be stronger than those between the molybdenum species and the silica surface. Bands appear at higher wavenumbers than ammonium paramolybdate because of the presence of larger aggregates of molybdenum. These species are also distorted, indicated by the bands shifted to lower wavenumbers in the 800 to 880 cm^{-1} region. Calcination of these compounds results in the formation of a "MoO_3" phase whose bands and relative intensities closely match those of the bulk compound. However, an aggregated species whose broad bands overlap those of the dried sample is present. The presence of this doublet structure clearly indicates a molybdenum environment for these stretching frequencies.

Addition of cobalt to the silica-supported samples indicates a more profound influence than for the alumina-supported samples. All samples indicate a stronger interaction of the cobalt with molybdenum. The presence of 930 to 935 cm^{-1} bands in the spectrum of the dried samples indicates close association of cobalt and molybdenum species; the band is also present in the calcined compounds. The presence of this phase dominates the spectrum of calcined samples, and the presence of "MoO_3" is apparent only at higher molybdenum loadings. The broad shoulders present on the "$CoMoO_4$" phase probably indicate the presence of aggregated molybdenum species associated with the "$CoMoO_4$" phase. The degree of interaction with the aggregated molybdenum species is most obvious in the spectra of the dried compounds. The low wavenumber data demonstrate that the cobalt breaks up the formation of an ordered molybdenum aggregate. Also apparent is the increase in smaller aggregates of molybdenum associated with cobalt by bands in the 800 to 850 cm^{-1} region of the spectrum. The order of impregnation dramatically affects the relative amounts of "$CoMoO_4$" and "MoO_3" formed. Impregnation of molybdenum first results in larger aggregates of molybdenum which persist in the calcined form. This phase is much less ordered and stoichiometric than the phase formed by simultaneous impregnation or cobalt impregnation first. A "Co_3O_4" phase is apparent in the spectra of these latter two methods of preparation. This phase is also clearly apparent in samples with lower loadings of molybdenum with the same level of cobalt present.

4c. Co–Mo/α-Al_2O_3 Catalysts

The low surface area and lack of reactivity of α-Al_2O_3 resulted in relatively simple spectra. A MoO_3 phase is present as well as $CoMoO_4$ and Co_3O_4 phases. Most of these phases show rather clear resemblance to bulk compounds. The relative concentration of the phases is independent of the order of impregnation.

REFERENCES

1. DeBeer, V. H. J., and Schuit, G. C. A., *in* "Preparation of Catalysts" (B. Delmon, P. A. Jacobs, and G. Poncelet, Eds.). Elsevier, Amsterdam, 1976.
2. Ahuja, S. P., Derrien, M. L., and LePage, J. F., *Ind. Eng. Chem. Prod. Res. Dev.* **9**, 272 (1970).
3. DeBeer, V. H. J., van der Aalst, M. J. M., Machiels, C. J., and Schuit, G. C. A., *J. Catal.* **43**, 78 (1976).
4. LoJacono, M., Schiavello, M., deBeer, V. H. J., and Minelli, G., *J. Phys. Chem.* **81**, 1583 (1977).
5. Villa, P. L., Trifiro, F., and Pasquon, I., *Reac. Kinet. Catal. Lett.* **1**, 341 (1974).
6. Brown, F. R., and Makovsky, L. E., *Appl. Spectrosc.* **31**, 44 (1977).
7. Brown, F. R., Makovsky, L. E., and Rhee, K. H., *J. Catal.* **50**, 385 (1977).
8. Medema, J., van Stam, C., de Beer, V. H. J., Konings, A. J. A., and Koningsberger, D., *J. Catal.* **53**, 386 (1978).
9. Cheng, C. P., and Schrader, G. L., "Laser Raman Spectroscopic Study of the Preparation of Cobalt Molybdate Catalysts." American Institute of Chemical Engineers National Meeting. Philadelphia, June 1978.
10. Ludowise, J. D., Cheng, C. P., and Schrader, G. L., *Appl. Spectrosc.*, submitted.
11. Cord, F. A., Courtine, P., and Pannetier, G., *Spectros. Acta* **28A**, 1601 (1972).
12. Abrahams, S. C., and Reddy, M. J., *J. Chem. Phys.* **43**, 2533 (1965).
13. Busey, R. H., and Keller, O. L., *J. Chem. Phys.* **41** (1), 215 (1964).
14. Lindqvist, I., *Arkiv Kemi* **2**, 349 (1950).
15. Shimao, E., *Bull. Chem. Soc. Japan* **40**, 1609 (1967).
16. Evans, H. T., *J. Amer. Chem. Soc.* **90**, 3275 (1968).
17. Jahr, K. F., and Fuchs, *J. Angew. Chem. Int. Edn.* **5**, 689 (1966).
18. Sasaki, Y., and Sillen, L. G., *Arkiv Kemi* **29**, 253 (1968).